

# Effects of Rotor Slot Area on Squirrel Cage Induction Motor Performance

Asim Gokhan Yetgin<sup>1</sup> and Mustafa Turan<sup>2</sup>

<sup>1</sup>Department of Electrical and Electronics Engineering, Dumlupinar University, Kutahya, 43100, Turkey

<sup>2</sup>Department of Electrical and Electronics Engineering, Sakarya University, Sakarya, 54000, Turkey

## Abstract

The Induction motors are the most widely used type of motor in the industry. Thus, induction motor design and control is of great importance. The effects of variation of the rotor slot area which is one of the most importance design parameters of the motor performance were examined. Change of the rotor slot area was examined in two ways. One of them, rotor slot height is changed. Second of them, rotor slot width is changed. Saturation, rotor resistance, efficiency etc. parameters are analyzed for two methods. 5.5 kW squirrel cage induction motor is used for modellings.

**Keywords:** Induction motor, Performance analysis, Rotor slot area, Slot height, Slot width.

## 1. Introduction

The design of the induction motor is a highly complex process. Many different variables such as output power, losses, efficiency, nominal torque, current etc. must be considered to obtain the desired motor parameter values. Stator and rotor slot structures, the type of sheet material, cooling-insulation-propeller etc. parameters must be designed/chosen in a good way.

Kim analyzed induction motor performance using three different rotor slot geometries [1]. Or and friends made vibration analyses of the induction motor which has same rotor area. They used rectangular and round rotor slot geometries for analyses. They obtained, the round rotor slot gives 4.8% less vibration than the rectangular rotor slot [2]. Dems and friend's paper present additional losses analysis of a three-phase induction motor with opened and closed rotor slots [3]. Lee and friends investigated torque-speed characteristic of the induction motor which has different rotor slot geometry [4]. Iqbal and Agarwal in their paper, examined performance of the induction motor. They used the three-different rotor geometry which has the same rotor area [5]. Virlan and friends analyzed four different rotor slot geometry which has same rotor geometry using Finite Element Method [6]. Maddi and

friends present the influence of the form of rotor slot on the startup characteristics of the induction motor [7]. Zhang and friends optimized round rotor slot geometry using Multi Objective Particle Swarm Optimization (MOPSO) [8]. The main goal of their paper is optimal design of a three-phase squirrel cage induction motor to increase efficiency and reduce the volume. For this purpose, the motor has been optimized by ant colony optimization algorithm offers maximum efficiency and minimum size [9]. Guldemir and Bradley look at the effect of different rotor slot designs on rotor slot harmonics in induction motor, line current and spectra [10].

In this paper, induction motor rotor slot area analyzed using two different methods. One of them, the rotor slot height is changed. Second of them, the rotor slot width is changed. Performance of the induction motor is obtained using two methods.

## 2. Induction Motor Design Procedure

The motor rating, stator current in phase, number of stator slots, air gap flux, turns of stator winding and stator induced voltage in phase is calculated as follows [9]:

$$S = \frac{P_{out}}{\eta * PF} \quad (1)$$

$$S = 0.95 * B_{av} * ac * K_{ws} * D^2 * L * n_s \quad (2)$$

where  $S$  is the motor rating in voltamperes,  $P_{out}$  is the motor output in wattage,  $\eta$  is the efficiency,  $PF$  is power factor,  $B_{av}$  is magnetic flux density,  $ac$  is the specific electrical loading in amperes per meter,  $K_{ws}$  is winding factor,  $L$  is the motor length in meters,  $D$  is the stator outer diameter in meters,  $n_s$  is the rated speed in revolutions per second.

$$I_s = \frac{S}{3 * V_{ph}} \quad (3)$$

$$S_s = 3 * q * p \quad (4)$$

$$\varphi = L_i * B_{av} * \tau_{ps} \quad (5)$$

$$N_{ph} = \frac{ac * \pi * D}{6 * I_s} \quad (6)$$

$$E_s = 4.44 * N_{ps} * \varphi * f * k_{ws} \quad (7)$$

$I_s$  is the stator current in phase,  $V_{ph}$  is the stator voltage in phase in volts,  $p$  is number of poles,  $q$  is the number of stator slots per pole per phase,  $S_s$  is the number of stator slots,  $\varphi$  is air gap flux/p,  $L_i$  is the real length of the motor in meters,  $\tau_{ps}$  is the stator pole pitch,  $N_{ph}$  is number of stator turns/phase,  $E_s$  is the stator induced voltage in phase in volts and  $f$  is frequency in hertz [9].

### 2.1 Rotor slot sizing

A lot of different rotor slot construction can use in the induction motor rotor slot type. These differences have an effect on motor performance in various ways. General rotor slot formulas are given below [11].

The value of rated rotor bar current  $I_b$ :

$$I_b = K_I * \frac{2 * m * N_{ph} * K_{ws} * I_s}{N_r} \quad (8)$$

$K_I=1$ , the rotor and stator mmf would have equal magnitudes. In reality, the stator mmf is slightly larger.  $N_r$  is rotor slot number,  $m$  is number of phase,  $J_b$  is rotor bar current density.

$$K_I \approx 0.8 * PF + 0.2 \quad (9)$$

The rotor slot area  $A_b$ :

$$A_b = \frac{I_b}{J_b} \quad (10)$$

The end ring current  $I_{er}$ :

$$I_{er} = \frac{I_b}{2 * \sin \frac{\pi * p}{N_r}} \quad (11)$$

The current density in the end ring  $J_{er}$ :

$$J_{er} = (0.75 - 0.8) * J_b \quad (12)$$

The end ring cross section  $A_{er}$ :

$$A_{er} = \frac{I_{er}}{J_{er}} \quad (13)$$

The motor rotor slot is given in Figure 1.

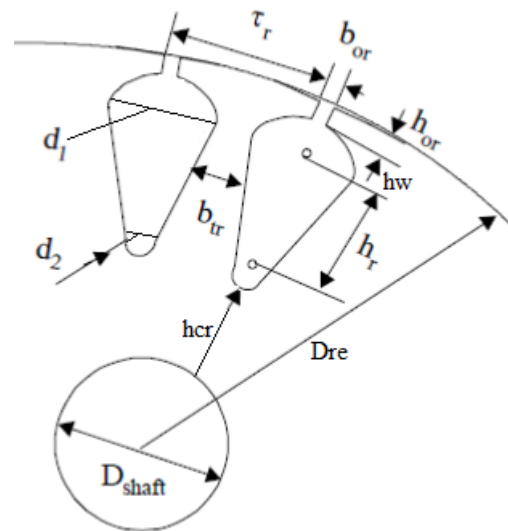


Figure 1. 5.5 kW induction motor's rotor slot geometry [11]

The rotor slot pitch  $\tau_r$  is,

$$\tau_r = \frac{\pi * (D_{is} - 2 * g)}{N_r} \quad (14)$$

The rotor tooth flux density  $B_{tr}$  is,

$$B_{tr} \approx \frac{B_g}{K_{fe} * b_{tr}} * \tau_r \quad (15)$$

The rotor back core flux density  $B_{cr}$  is,

$$B_{cr} = \frac{\phi}{2 * L * h_{cr}} \quad (16)$$

The rotor slot area can be also calculated using rotor slot parameters.

$$A_b = \frac{\pi}{8} * (d_1^2 + d_2^2) + \frac{(d_1^2 + d_2^2) * h_r}{2} \quad (17)$$

In the formulas,  $D_{is}$  is the stator inner diameter,  $g$  is the air-gap length,  $B_g$  is the air-gap flux density,  $b_{tr}$  is the rotor tooth width,  $h_{cr}$  is the rotor back iron height.

Size value of short-circuit rings, cross section internal diameter must be known for calculate the rotor resistance.  $k_{dr}$  and  $k_{pr}$  present the rotor distribution coefficient and rotor chording factor respectively and they are calculated as in the stator [12].

$$R_r = 1.169 * 10^{-6} * \left( \frac{k_{w1} * W_1}{k_{dr} * k_{pr}} \right)^2 * \left( \frac{1}{N_r * A_b} + \frac{2}{\pi} * \frac{D_{er}}{p^2 * A_{er}} \right) \quad (18)$$

The rotor leakage reactance value is calculated as follows equivalent 19 [11].  $X_{be}$  is the equivalent rotor bar leakage reactance.

$$X_r = 4 * m * \frac{(w_1 * K_{ws})^2}{N_r} * X_{be} \quad (19)$$

The other induction motor design parameters given in reference [11, 12].

### 3. Obtained Values

#### 3.1 Change of height

In this section, rotor slot height parameter is changed. Performance evaluation was conducted according to the new slot areas. The rotor slot height is changed from 10 mm to 21 mm. Change of the rotor leakage reactance and rotor resistance values versus the rotor area are given in Figure 2.

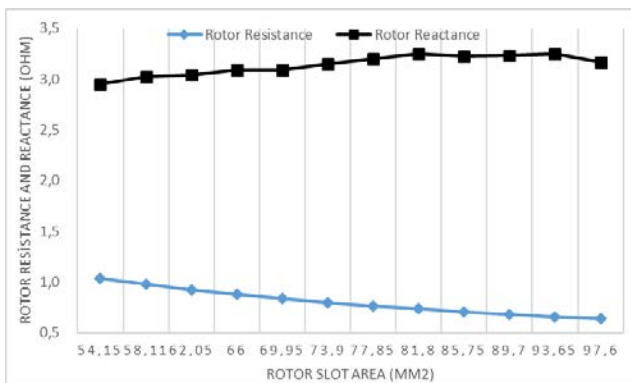


Figure 2. Rotor resistance and reactance versus rotor slot area

The Figure 2 is examined, it is seen that the rotor slot area increased the rotor resistance is decreased and rotor leakage reactance value is increased. Magnetic field values at the rotor back iron and between the rotor teeth are given in Figure 3.

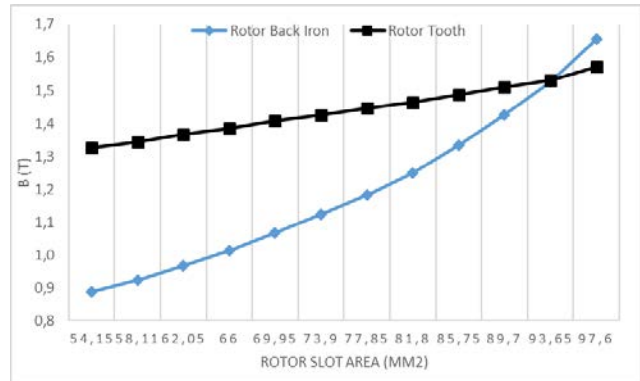


Figure 3. Magnetic field distribution versus rotor slot area

When Figure 3 is investigated, rotor back iron part height value is decreased while rotor slot height is increased. Depending upon this effect, value of magnetic field density is increased.  $B$  value raise between rotor teeth is observed. Rotor copper losses is given in Figure 4.

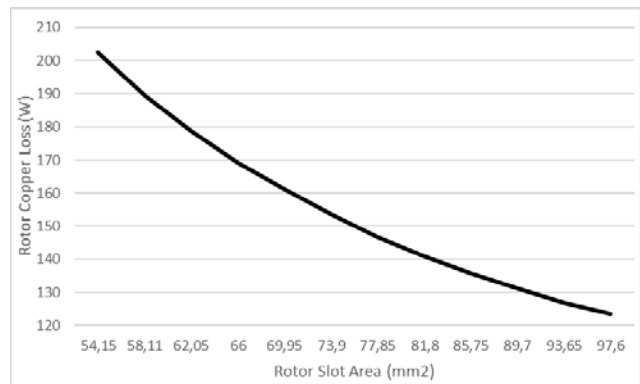


Figure 4. Rotor copper loss versus rotor slot area

It is observed that rotor copper losses are decreased at a great rate if rotor area is increased. Reason of this decrease is that rotor bar current stays steady and rotor resistance is decreased by half. Motor efficiency change with respect to rotor area is shown in Figure 5.

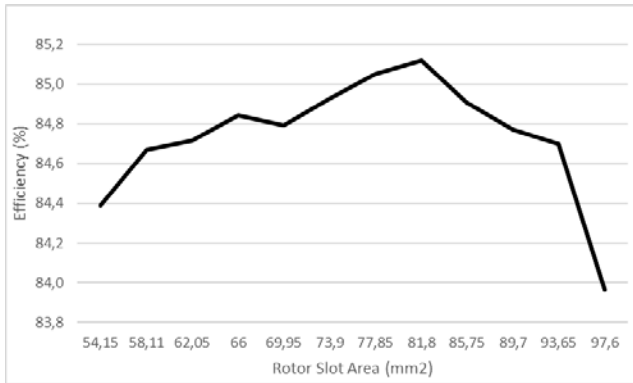


Figure 5. Efficiency versus rotor slot area

When Figure 5 is investigated, small changes in iron losses and differences in input power leads to raise in efficiency up to certain value and then decrease.

### 3.2. Change of width

In this section, one of the rotor slot parameters, slot upper width value is changed. Performance evaluation is performed up to new rotor areas. The rotor slot upper width is changed from 4 mm to 7.4 mm. Rotor resistance and rotor leakage reactance change with respect to rotor area is given in Figure 6.

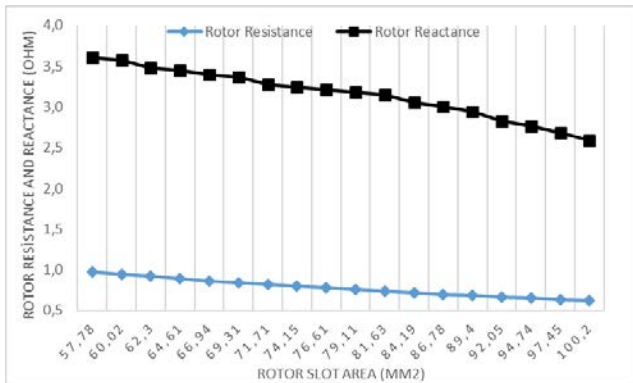


Figure 6. Rotor resistance and reactance versus rotor slot area

It is seen that rotor resistance graph is obtained similar to height change. Leakage reactance value is acquired the exact opposite. Magnetic field distribution in rotor teeth and rotor back iron part with respect to rotor area is depicted in Figure 7.

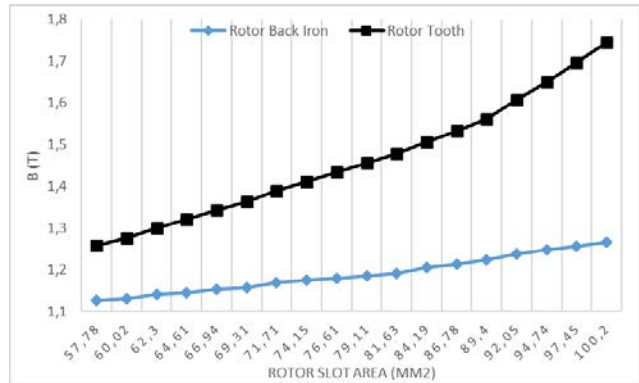


Figure 7. Magnetic field distribution versus rotor slot area

When Figure 7 is investigated, a graph is obtained similar to the values acquired from height change. Rotor copper loss and efficiency graphs are given in Figure 8 and Figure 9.

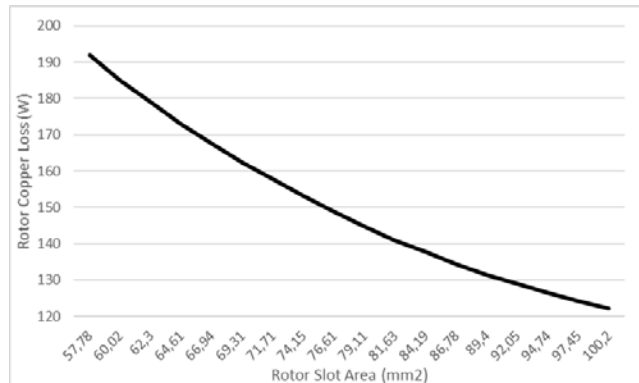


Figure 8. Rotor copper loss versus rotor slot area

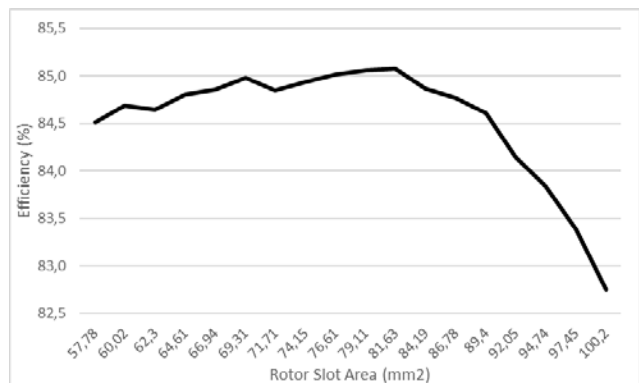


Figure 9. Efficiency versus rotor slot area

Results obtained from both of the graphs look like the outcomes from rotor slot height change.

## 4. Conclusions

In this study, effect of rotor slot area induction machine performance is examined. Two methods are handled for rotor area change. In the first one, rotor slot height is changed. In the second one, rotor slot width is changed. Performance evaluation is performed for both studies.

When efficiency change is investigated for both, results look like bell curve shaped. This situation shows that rotor area must be chosen optimally.

## References

- [1] Y. S. Kim, “Analysis of Starting Torque and Speed Characteristics for Squirrel Cage Induction Motor According to Material Properties of Rotor Slot”, *Transactions on Electrical and Electronic Materials*, Vol. 16, No. 6, 2015, pp. 328-333.
- [2] P. P. L. Or, S. Peaiyoung, T. Kulworawanichpong, and S. Sujitjorn, “Effects of the Geometry of the Rotor Slots on the Mechanical Vibration of Three-phase Induction Motors”, *Proceedings of the 7th WSEAS International Conference on Simulation, Modelling and Optimization*, Beijing, China, September 15-17, 2007, pp. 434-438.
- [3] M. Dems, K. Komez, S. Wiak, and S. F. Coya, “Influence of the Closing Rotor Slots on the Additional Losses in the Induction Motor”, *COMPEL: The International Journal for Computation and Mathematics in Electrical and Electronic Engineering* Vol. 34 No. 2, 2015 pp. 531-549.
- [4] G. Lee, S. Min, and J. P. Hong, “Optimal Shape Design of Rotor Slot in Squirrel-Cage Induction Motor Considering Torque Characteristics”, *IEEE Transactions on Magnetics*, Vol. 49, No. 5, 2013, pp. 2197-2200.
- [5] M. A. Iqbal and V. Agarwal, “Investigation & Analysis of Three Phase Induction Motor Using Finite Element Method for Power Quality Improvement”, *International Journal of Electronic and Electrical Engineering*. Vol. 7, No 9, 2014, pp. 901-908.
- [6] B. Virlan, A. Simion, L. Livadaru, A. Munteanu, A. M. Mihai, and S. Vlasceanu, “External Rotor Shape Estimation of an Induction Motor by Fem Analysis”, *Buletinul AGIR* nr. Vol. 4, 2011, pp. 27-32.
- [7] Z. Maddi, D. Aouzellag, and T. Laddi, “Influence of the Skin Effect and the Form of Slot on the Starting Characteristics of Induction Motor Squirrel Cage”, *Recent Advances in Mechanics, Mechatronics and Civil, Chemical and Industrial Engineering*, 2015, pp. 125-129.
- [8] D. Zhang, Z. Ren and C. S. Koh, “Multi-Objective Optimal Design of a NEMA Design D Three-phase Induction Machine Utilizing Gaussian-MOPSO Algorithm”, *Journal Electrical Engineering and Technology*, Vol. 9, No. 1, 2014, pp. 184-189.
- [9] B. Alizadeh and S. A. Gholamian, “Application of Ant Colony Optimization Algorithm for Optimal Design of Squirrel Cage Induction Motor”, *International Journal of Mechatronics, Electrical and Computer Technology* Vol. 4, No. 13, 2014, pp. 1674-1690.
- [10] H. Guldemir, and K. J. Bradley, “The Effect of Rotor Design on Rotor Slot Harmonics in Induction Machines”, *Electric Power Components and Systems*, Vol. 29, No. 9, 2001, pp. 771-788.
- [11] I. Boldea, and S. A. Nasar, *The Induction Machine Handbook*, CRC Pres LLC, Washington, D.C., 2002.
- [12] J. J. Cathey, *Electric Machines Analysis and Design Applying Matlab*, Mc Graw-Hill, 2001.

**Asim Gokhan Yetgin** was born in Kutahya, Turkey, in 1979. He received the BSc and MSc degrees in 2001 and 2004 from the Department of Electrical Electronics Engineering, Selcuk University, Konya, Turkey and Dumlupinar University, Kutahya, Turkey respectively. He received PhD degree from Sakarya University. He is working as Assistant Professor in Department of Electrical Electronics Engineering, Dumlupinar University. His areas of research include optimization, design and modeling of electrical machines, finite element method and energy saving.

**Mustafa Turan** was born in Babaeski, Turkey, in 1964. He has received BS degree from Istanbul Technical University, MSc and PhD degrees from Sakarya University, Turkey in the years 1987, 1994 and 2002 respectively, in Electrical Engineering. He is a faculty member of Electrical and Electronics Engineering Department, Sakarya University, Turkey, since 2002, and currently serving as Assistant Professor. His research interests include design, performance analysis and optimization of electrical machines, power quality power system stability.